Liquid Crystals
Publication details, including instructions for authors and subscription information:
http://www.tandfonline.com/loi/tlct20

Analysis of the rotation of the polarisation direction in a cylindrical liquid crystal lens where the direction of the incident linear polarisation is not parallel to the axis of the cylindrical lens

HyungKi Hong [a]

[a] Department of Visual Optics, Seoul National University of Science and Technology, Nowon-gu, Seoul, Republic of Korea

Available online: 20 Oct 2011

Liquid Crystals,
Vol. 39, No. 2, February 2012, 157–164

Taylor & Francis
Taylor & Francis Group

Analysis of the rotation of the polarisation direction in a cylindrical liquid crystal lens where the direction of the incident linear polarisation is not parallel to the axis of the cylindrical lens

HyungKi Hong*

Department of Visual Optics, Seoul National University of Science and Technology, Nowon-gu, Seoul, Republic of Korea

(*Received 13 July 2011; final version received 2 September 2011*)

A liquid crystal (LC) lens is used to change the propagating direction of the incident light at the lens-shaped boundary of two different media and shows strong dependence on the polarisation direction of the incident light. The performance of the cylindrical LC lens is investigated in the situation that the directions of the incident linear polarisation and the axis of the cylindrical lens are not parallel. Two LC cell configurations were considered where LC directors aligned twisted or homogeneously. In case of the twisted LC configuration, the polarisation direction of the propagating light follows the twist of the LC directors if the directions of the incident linear polarisation and the LC alignment on the side of the lower substrate are parallel. For these two configurations, the LC lens can control the propagating light in the LENS-ON state. In case of homogeneously aligned LC configuration, polar angle distributions of LC directors are not uniform due to the lens-shaped boundary. So in the LENS-OFF state where LC directors rotate under the driving voltage, a LC domain boundary may occur in some cases.

Keywords: liquid crystal (LC) lens; cylindrical; polarisation; autostereoscopic 3D

1. Introduction

Three-dimensional (3D) technology is gaining attention in 3D theatre and 3D TV [1–4]. Among the various types of 3D methods, current technology is focusing on a 3D method using a special eyeglass. Yet, it is expected that an autostereoscopic 3D method where the viewer does not need a special eyeglass to perceive the binocular depth will eventually replace 3D method using the special eyeglass. In autostereoscopic 3D using a lens sheet of cylindrical lens arrays, the lens sheet is placed in front of the imaging display to control the direction of the light coming from the imaging display. As the users watch a two-dimensional (2D) image as well as a 3D image, switching between 2D and 3D modes is necessary for the wider acceptance of autostereoscopic 3D display. For this purpose, various switching methods have been reported such as changing the refractive index of the liquid crystal (LC) at the lens-shaped boundary or controlling the spatial distribution of the refractive index to match the phase profile of the geometric lens [5–12].

One of reported switching methods is the control of the refractive index at the lens-shaped boundary such that the difference in the refractive index of two adjacent media determines the characteristics of the switching lens as illustrated in Figure 1 [9, 10]. The direction of homogenous LC alignment and the axis of the cylindrical lens are parallel. The refractive index of the transparent isotropic medium is the same as n_o, the refractive index of liquid crystal for ordinary wave. When the linear polarisation of the y-axis direction is incident on this structure, the refractive index difference at the lens-shaped boundary causes the change in propagating direction. When LC directors are aligned vertically by the driving voltage, the refractive index difference at the lens-shaped boundary is zero and the propagating direction does not change at the lens-shaped boundary. However, this structure cannot be used as the lens for the incident linear polarisation in the x-axis direction. Therefore, if the polarisation direction of the incident light is not along the y-axis direction, the propagating directions of some of the incident light will not be controlled by the LC lens.

It often happens that the polarisation direction of the incident light is not parallel to the axis of the cylindrical lens [11, 13–15]. In that situation, it is no longer guaranteed that all of the incident light will change propagating direction at the lens-shaped boundary. Therefore, the change in incident polarisation inside the LC cell of the LC lens needs to be investigated to estimate the behaviour of the propagating light at the lens-shaped boundary. In this paper, for a LC lens using the cylindrical lens-shaped boundary, two LC cell configurations are considered where LC directors align twisted or homogenously. Changes in the incident linear polarisation are investigated for various LC cell conditions to find the condition where all of the incident light changes propagating direction at the lens-shaped boundary.

*Email: hyungki.hong@snut.ac.kr

ISSN 0267-8292 print/ISSN 1366-5855 online

http://dx.doi.org/10.1080/02678292.2011.620991
http://www.tandfonline.com

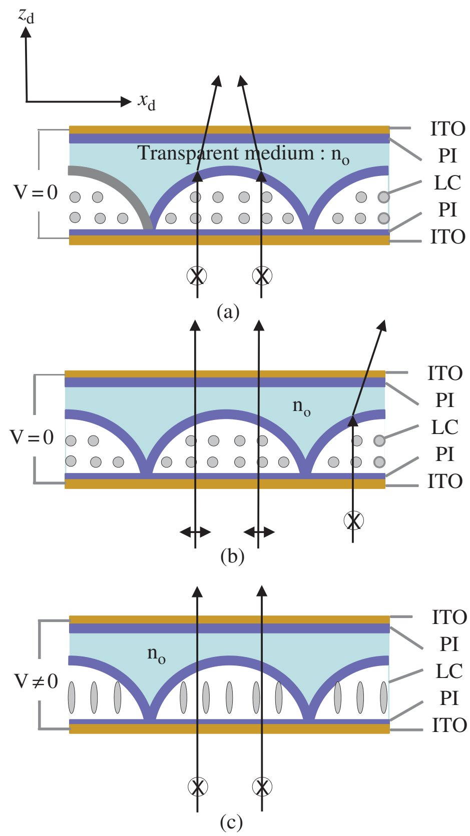

Figure 1. Example of LC lens where the boundary between the LC layer and the transparent medium is lens-shaped. (a) At zero voltage, the linear polarisation of the *y*-axis direction changes the propagation direction at the lens-shaped boundary due to the difference in the refractive index. (b) At zero voltage, the linear polarisation of the *x*-axis direction does not change the propagation direction. (c) At non-zero voltage, the linear polarisation of the *y*-axis direction passes through the lens-shaped boundary without changing the propagating direction. ITO, PI and LC represent indium tin oxide, polyimide and liquid crystal respectively. Circled X and double-sided arrow represent the linear polarisation of the *y*-axis direction and the *x*-axis direction respectively. The directions of the *x*-axis and the *z*-axis are represented on the left upper side of the figure.

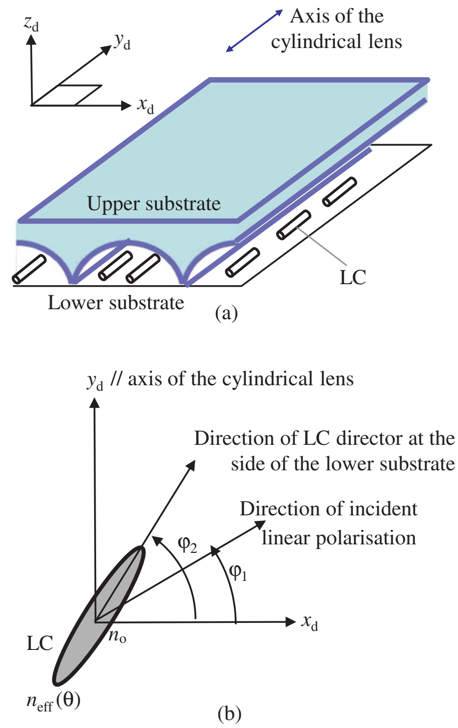

Figure 2. (a) Structure of the cylindrical LC lens. Electric field exists along the *z*-axis direction. (b) Notation of angles and directions. Cylinders represent LC directors.

2. Theory

Polarisation of the incident light and the axis of the cylindrical lens are not always parallel. Some of such examples are 2D/3D switchable autostereoscopic 3D [11, 13–15].

To investigate the polarisation change inside a LC lens, the cylindrical lens illustrated in Figure 2(a) is considered. The lens radius is selected to be infinite along the *y*-axis direction. The axis of the cylindrical lens is defined as parallel to the *y*-axis direction. The incident light is assumed to propagate along the *z*-axis. Notations of the direction of LC director and the incident polarisation are illustrated in Figure 2(b).

Linear polarisations along the *x*-axis and the *y*-axis directions are defined as P1 and P2 respectively. In the case of the cylindrical LC lens where LC directors align homogeneously along the *y*-axis direction, the cylindrical LC lens can change the propagating direction of the P2 component of the incident light but not the direction of the P1 component. Hence, the propagating direction of some of the incident light may not be changed at the cylindrical LC lens. To prevent this, it is necessary to investigate the LC cell configuration and the polarisation direction inside the LC cell together.

In the phenomenon called 'adiabatic following' it is known that the direction of the incident polarisation rotates with the twist of LC directors [16, 17]. The rotation of the linear polarisation along the LC director is illustrated in Figure 3. This phenomenon occurs when the change of LC twist is small enough compared with the overall phase retardation Γ of the LC cell and the polarisation direction of the incident light is parallel or perpendicular to the LC director on the side of incident direction. This adiabatic following phenomenon is reported for the LC cell of the planar boundary but not for the non-planar boundary (like the lens-shaped boundary). Thus it needs to be investigated whether the concept of the adiabatic following phenomenon is still effective for the LC cell of the lens-shaped boundary. And if this concept is

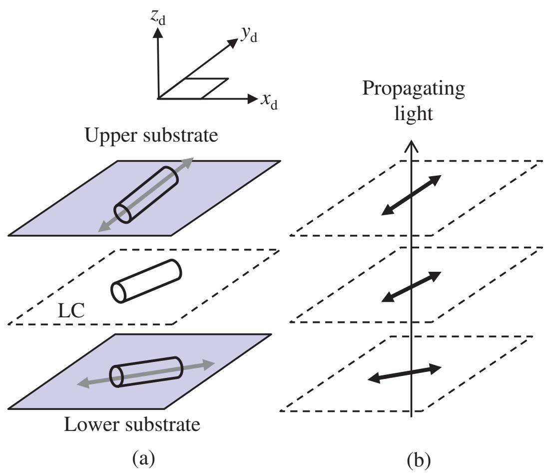

Figure 3. Phenomenon of adiabatic following. (a) Alignment of LC directors. Double-sided grey arrows and cylinders represent the rubbing direction and LC directors. (b) Direction of propagating linear polarisation through LC cell. Double-sided black arrows represent the direction of the linear polarisation.

effective, the incident linear polarisation whose direction is not parallel to the axis of the cylindrical lens could be rotated inside the LC cell to be parallel to the axis of the cylindrical lens. Then there would be no light that does not change propagating direction at the lens-shaped boundary. Therefore the possibility of using the twisted LC configuration for the LC lens is investigated.

In the case where the direction of LC cell of homogeneous alignment is parallel with the incident linear polarisation, the incident light will propagate through the LC layer to the lens-shaped boundary. In addition, the distribution of LC directors at the lens-shaped boundary will determine the change of the propagating direction. In this configuration, the distribution of LC directors needs to be investigated in detail.

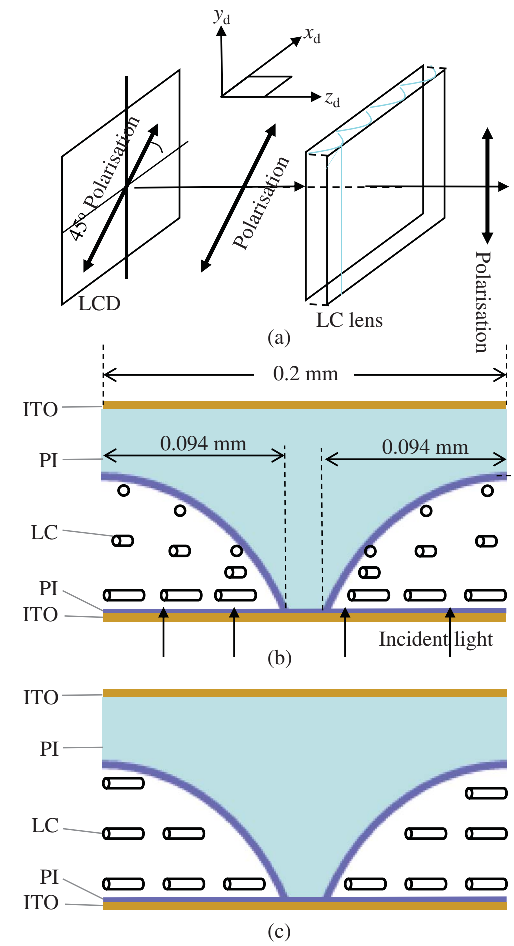

Figure 4. (a) Schematic of autostereoscopic 2-view 3D. Azimuth angle of the incident polarisation direction and the axis of the cylindrical lens are 45° and 90°. (b) Configuration of the cylindrical LC lens using the twisted LC alignment. The axis of the cylindrical lens and the LC alignment direction are parallel at the upper side of LC cell but are not parallel at the lower side of LC cell. (c) Configuration of cylindrical LC lens using the homogeneous LC alignment. Cylinders represent LC directors. ITO, PI and LC represent indium tin oxide, polyimide and liquid crystal respectively.

3. Simulation

The cylindrical LC lens using the twisted LC alignment or the homogeneous LC alignment was investigated to design a LC lens that could be used for the situation where the axis of the cylindrical lens and the direction of the incident linear polarisation are not parallel. The LC cell configuration of the twisted LC alignment as well as the homogeneous LC alignment were designed and the LC distribution was calculated using commercial software (TechWiz 2D) [18]. The state of each linear polarisation at the lens-shaped boundary will determine whether the propagation direction changes or not. The intensity and the phase retardation of each linear polarisation at the lens-shaped boundary were also calculated from the calculated LC director distribution.

In selecting the cylindrical lens condition for the calculation, an autostereoscopic 2-view 3D display is considered as an example, as illustrated in Figure 4(a). A liquid crystal display (LCD) of RGB (red/green/blue) subpixel configuration of vertical stripe type and subpixel pitch of around 0.1 mm and polarisation direction of 45° was considered as the imaging display. The focal lens f is selected as 1.7 mm. The interpupilar distance (IPD) between the eyes is known to be 65 mm for adults. The lens pitch P_{lens} of each cylindrical lens is selected as 0.2 mm. The designed viewing distance is determined as f (1 + 2

IPD / P_{lens}) [2]. This corresponds to the designed viewing distance of 1100 cm for autostereoscopic 2-view display.

Figure 4(b) illustrates the configuration of the LC lens using the twisted LC cell designed for the simulation. The infinite length is assumed to be along the *y*-axis direction. Therefore, the LC distribution along the *y*-axis direction is not considered. The period of the horizontal size is selected as 0.2 mm and the periodic boundary condition is used along the *x*-axis direction. The pretilt angle for the upper and the lower side are selected as 4°. For the simulation, the refractive index of LC is selected as n_e=1.5977 and n_o=1.4828. From the product of the focal length and the difference of refractive index, the radius of the lens pattern is determined to be 0.149 mm. For the lens pitch of 0.2 mm, the thickest region of the LC layer is 0.033 mm – as illustrated in Figure 4(b). The lens pattern on the upper substrate contacts the lower substrate at a position 0.094 mm from the left horizontal boundary of the LC cell. Other material parameters of the LC are selected such that dielectric constants are $\varepsilon_e = 8.3$ and $\varepsilon_o = 3$, the elastic constants are $K_{11} = 13$ pN, $K_{22} = 5.8$ pN, $K_{33} = 12.7$ pN. The alignment direction at the lens pattern on the side of the upper substrate is selected as an azimuth angle of 90°, parallel to the axis of the cylindrical lens. The alignment direction of the side of the lower substrate is selected as an azimuth angle of 45°.

Figure 4(c) illustrates the other configuration of the LC lens where LC directors align homogeneously. The condition of the azimuth angle of the LC alignment is varied. The driving voltage is applied by two indium tin oxide (ITO) electrodes on the lower and upper sides of the substrates.

4. Results and analysis

LC director distributions and the state of the incident linear polarisation through the LC lens were obtained for the two LC lens configuration and the calculation conditions described in Section 3.From these calculated results, the performances of these two configurations were analysed.

Figure 5 illustrates the calculated result of the LC directors for the cylindrical LC lens of 45° twisted LC alignment as described in Figure 4(b) at a driving voltage of 0 V. Figure 5(a) shows the graphical representation of the LC directors. The contour maps of the azimuth angle and polar angle of LC director distributions are illustrated in Figures 5(b) and 5(c). As the boundary on the upper side is lens-shaped, the polar angle distribution deviates from the pretilt angle of 4°. Figure 6(a) shows the normalised intensity of P1 and P2 at the lens-shaped boundary for the

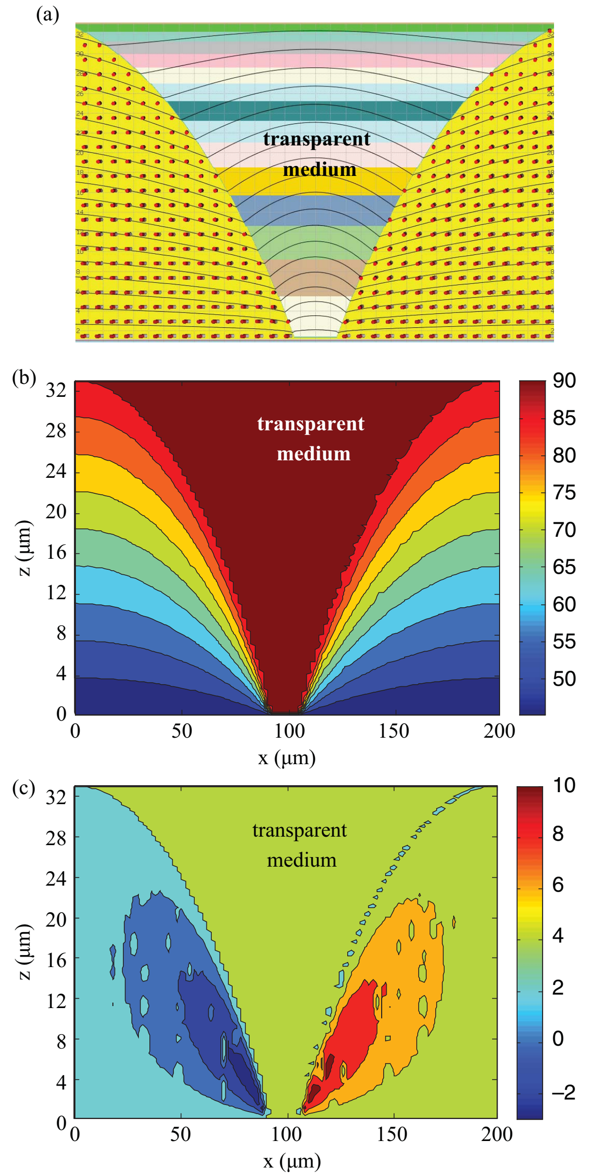

Figure 5. Calculated result of cylindrical LC lens of 45° twist under the driving voltage of 0 V. (a) Distributions of LC directors. (b) Contour map of the azimuth angle ϕ of LC director distribution. (c) Contour map of the polar angle θ of LC director distribution. The horizontal and vertical axes represent the position of the *x*-axis and *z*-axis respectively. Though there is no LC director inside the transparent medium on the side of the upper substrate, this region is represented by the initial rubbing condition of ϕ=90° and $\theta = 4°$.

calculated result of Figure 5 when the azimuth angle ϕ_1 of the incident linear polarisation is 45°, parallel to the alignment direction of the LC at the side of the lower substrate. P1 and P2 represent the linear polarisation of the *x*-axis and the *y*-axis directions. Hence, the azimuth angles of these polarisations are 0° and 90° respectively. The normalised intensity of

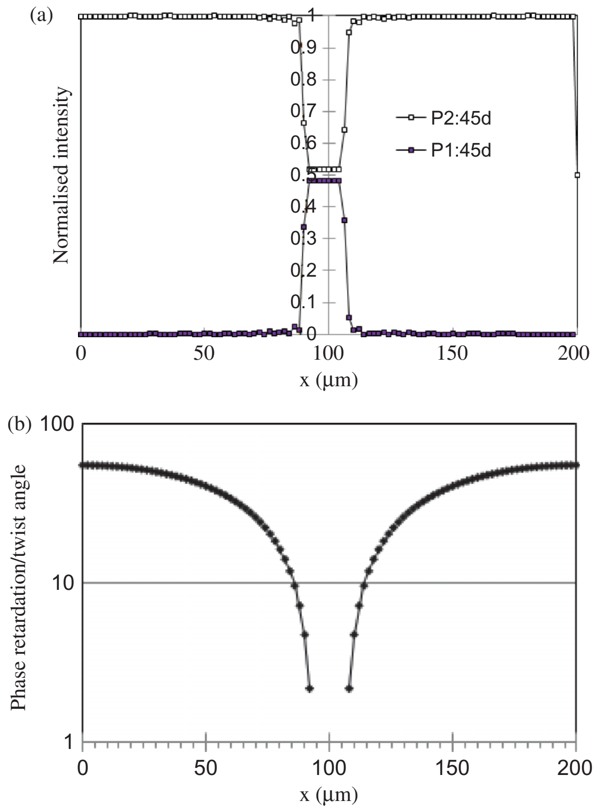

Figure 6. (a) Calculated normalised intensity of linear polarisation P1 and P2 after passing through LC lens of 45° twist when the azimuth angle of the incident linear polarisations is 45°. P1 and P2 represent the linear polarisation of the *x*-axis and the *y*-axis directions. (b) Calculated phase retardation divided by the twist angle in the LC lens cell. Horizontal axis represents the distance from the left boundary of the LC lens.

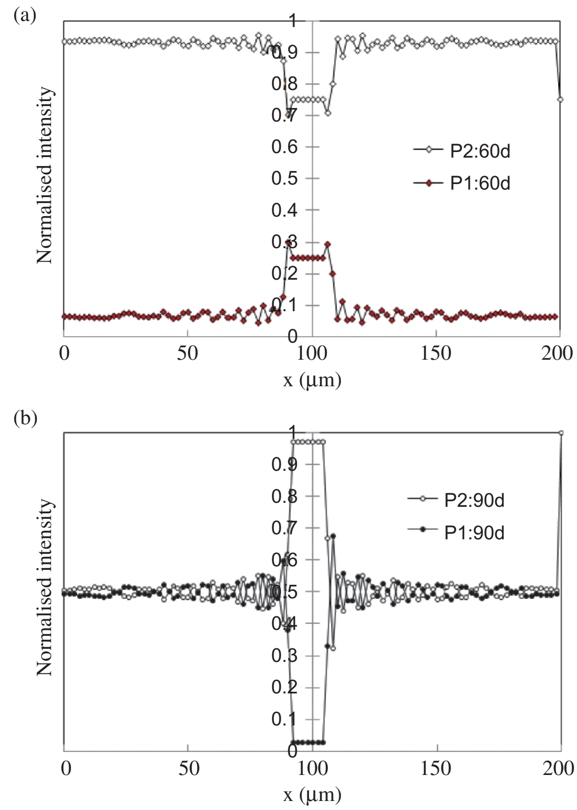

Figure 7. Normalised intensity of linear polarisation P1 and P2 after passing through LC lens of 45° twist when the azimuth angle of the incident linear polarisations is (a) 60° and (b) 90°. P1 and P2 represent the linear polarisation of the *x*-axis and the *y*-axis directions. Horizontal and vertical axes represent the horizontal position and the normalised intensity respectively.

P2 is one, meaning that the incident linear polarisation of the azimuth angle of 45° rotates inside the LC cell and becomes the linear polarisation of the azimuth angle of 90° at the lens-shaped boundary. The intensity of P1 is almost zero except in the region where the horizontal positions are 90–110 μm. Figure 6(b) illustrates the ratio between the phase retardation and the twist angle. The adiabatic following is initially assumed to occur when this ratio is large enough than 1. So, the assumption is that the adiabatic following will not hold in the horizontal positions between 90 and 110 μm where the distance between the lens-shaped boundary and the lower substrate is small. Apart from this region, the incident linear polarisation of the azimuth angle of 45° becomes P2 polarisation at the lens-shaped boundary and therefore will change the propagating direction. While P1 component will pass through the lens-shaped boundary without a change of propagating direction, the intensity of P1 becomes negligible by the LC cell.

Figure 7 illustrate the normalised intensity of P1 and P2 at the lens-shaped boundary for the calculated result of Figure 5 when the direction of the incident linear polarisation is not parallel with the LC alignment on the side of the lower substrate. In Figure 7, the normalised intensity of P1 increases as the azimuth angle φ_1 of the incident linear polarisation is farther from the azimuth angle $\varphi_2 = 45°$ of LC alignment direction on the lower substrate. That means that the incident polarisation decomposes into two components, which are perpendicular or parallel to the LC alignment on the side of the lower substrate. In addition, these two components rotate with the LC twist respectively. Hence each intensity of the P1 and P2 components at the lens-shaped boundary can be written as:

$$\sin^2(\varphi_1 - \varphi_2) \text{ and } \cos^2(\varphi_1 - \varphi_2) \qquad (1)$$

These calculated normalised intensities for the twisted LC configuration imply that the linear polarisation follows the LC twist as predicted by the assumption of the adiabatic following when the LC layer is thick enough. And that the propagating direction of the incident light can be controlled by the LC lens even when direction of the incident linear polarisation is not parallel to the axis of the cylindrical lens. Matching the direction of the incident polarisation and LC alignment on the lower substrate is necessary to obtain the linear polarisation parallel to the axis of the cylindrical lens at the lens-shaped boundary by the adiabatic following.

Figure 8 illustrates the calculated result of LC directors for the LC lens where the LC directors align homogeneously at an azimuth angle of 45°. The contour map of the azimuth angle distribution shows that the azimuth angles of LC directors are mostly 45°. Hence, the direction of the incident linear polarisation of the azimuth angle of 45° will be little affected as light passes through the LC layer. This light will change the propagating direction at the lens-shaped boundary.

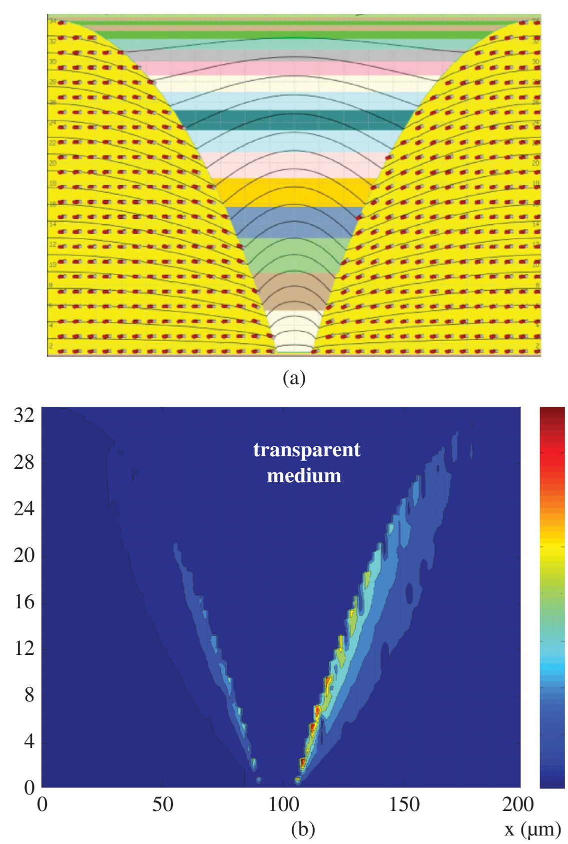

Figure 8. Calculated result of LC lens of homogeneous alignment of azimuth angle $\varphi = 45°$ under the driving voltage of 0 V. (a) Distribution of LC directors. (b) Contour map of the azimuth angle φ of LC director distribution. Horizontal and vertical axes represent the position of the x-axis and z-axis respectively.

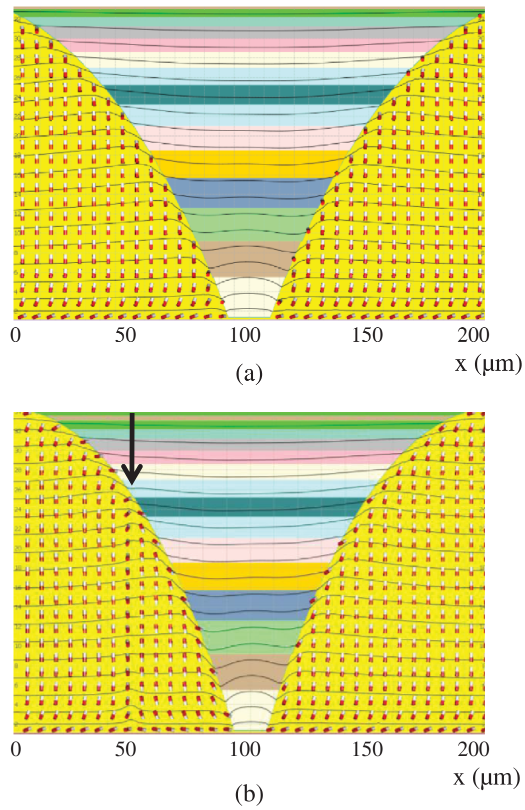

Figure 9. Distribution of LC directors under the driving voltage of 5 V for the LC lens using the LC cell of (a) 45° twist and (b) homogeneous alignment of azimuth angle $\varphi = 45°$. Arrow represents the position of the domain boundary. Horizontal and vertical axes represent the position of the x-axis and z-axis respectively.

To be useful as the switching lens, the characteristics of the LENS-OFF state are also important. Figure 9 illustrates the calculated distribution of LC directors under a driving voltage of 5 V for the LC lens configurations of Figures 4(b) and 4(c). When the electric field is applied along the z-axis direction, the LC directors rotate to the direction of the z-axis. As the refractive index difference at the lens-shaped boundary becomes zero, the LC lens becomes the LENS-OFF state. In the case of the LC lens of 45° twist, the LC directors behave as one domain as illustrated in Figure 9(a). In the case of the LC lens of homogeneous alignment of the azimuth angle of 45°, two rotating directions of LC directors appear and the domain boundary exists on the left side as illustrated in Figure 9(b). The polarisation state near the domain boundary is difficult to control and may affect the performance of the LENS-OFF state.

Figure 10 illustrates the calculated distribution of LC directors under a driving voltage of 5 V for

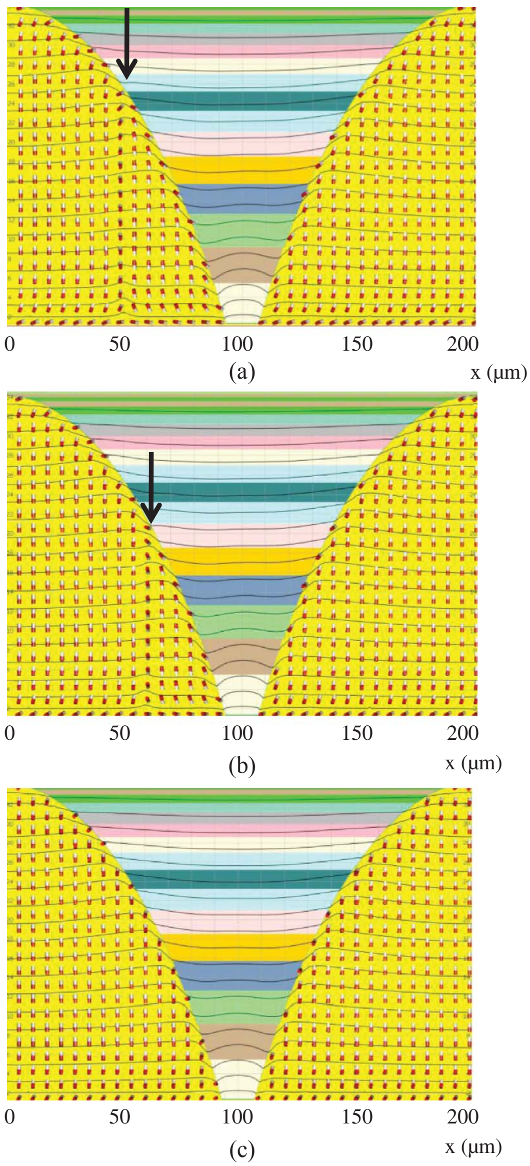

Figure 10. Distribution of LC directors under the driving voltage of 5 V for the LC lens using the LC cell of homogeneous alignment where azimuth angle ϕ is (a) 45° (b) 60° and (c) 90°. Arrows represent the position of the domain boundary. Horizontal and vertical axes represent the position of the x-axis and z-axis respectively.

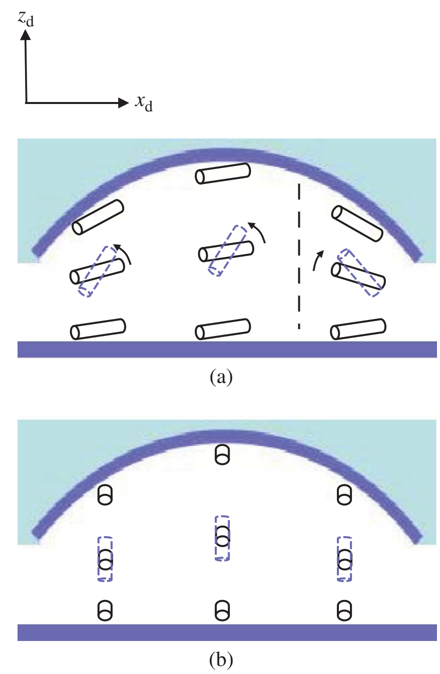

Figure 11. Schematic representation of the distribution of LC directors due to the lens-shaped boundary where the azimuth angle of the homogeneous alignment is (a) smaller than 90° and (b) 90°. Cylinders represent LC directors. Dotted cylinders represent the LC directors under the driving voltage. The one-sided arrow represents the rotation direction of LC directors under the driving voltage. The dotted line represents the position of the domain boundary. Dotted cylinders represent the LC directors under the driving voltage.

the LC lens configurations of homogeneous alignment at a different azimuth angle. As the azimuth angle increases from 45° to 60°, the domain boundary moves to the position where the surface curvature of the upper boundary is steeper. At the azimuth angle of 90°, the domain boundary does not occur. Figure 11(a) schematically illustrates the LC directors of the homogenous alignment when the azimuth angle of LC director is not 90°. It shows that, due to the lens shaped boundary of the upper side, the polar angles of the LC directors inside the LC cell are not equal to the pretilt angle. In addition, the sign of the tilt directions of the LC directors inside the LC cell at zero voltage is different for the left and the right side. Therefore, these LC directors of different signs will rotate along different directions under the driving voltage and form two domains. Figure 11(b) illustrates the LC directors of the homogenous alignment when the azimuth angle of the LC director is 90°. As the radius of the cylindrical lens is infinite along the axis of the cylindrical lens that is the y-axis direction, the polar angles of the LC directors inside the LC cell are equal to the pretilt angle. Hence, all LC directors rotate to the same direction under the driving voltage and form one domain. Therefore, the domain boundary tends to appear at the LENS-OFF state if azimuth angle of homogeneously aligned LC directors is not parallel to the axis of the cylindrical lens.

While the calculation is performed only for the limited conditions of azimuth angles, the trend obtained at this condition will be useful for the other value of φ_1. LC configurations of the cylindrical LC lens and their performance are summarised in Table 1.

Table 1. Comparison of LC lens of the different LC configurations where the azimuth angle of the incident linear polarization and the axis of the cylindrical lens are different.

LC configuration	Lens On	Lens Off
Homogenous alignment $\varphi_4 = \varphi_2 = \varphi_3$	Propagating direction of $\sin^2(\varphi_1 - \phi_2)$ intensity of the incident light is not changed	No domain boundary
Homogenous alignment $\varphi_1 = \varphi_2 = \varphi_3$	Propagating direction of all intensity of the incident light is changed	Possibility of domain boundary
Twisted alignment $\varphi_1 = \varphi_2$ and $\varphi_3 = \varphi_4$	Propagating direction of all intensity of the incident light is changed.	No domain boundary

φ_1: azimuth angle of direction of incident linear polarization
φ_2: azimuth angle of directionof LC director at the side of the lower substrate
φ_3: azimuth angle of direction of LC director at the side of the upper substrate
φ_4: azimuth angle of direction of axis of the cylindrical lens

5. Conclusions

Two LC configurations of the cylindrical LC lens are considered for the situation where the directions of the incident polarisation and the axis of the cylindrical lens are not parallel. As for LC lens using the twisted LC configuration, the propagating direction of the incident light can be controlled if the directions of the incident polarisation and the LC alignment on the side of the lower substrate are parallel. At the LENS-OFF state induced by the vertical electric field, LC directors rotate only along the one direction. As for the LC lens using the homogenous alignment, the propagating direction of all of the incident light can be controlled if the directions of the incident polarisation and the homogenous LC alignment are parallel. Yet, at the LENS-OFF state induced by the vertical electric field, the lens-shaped boundary can cause the domain boundary in some cases. Hence, the non-existence of the domain boundary needs to be considered as well.

The twisted LC configuration or homogeneous LC alignment is known to possess viewing angle dependence. In applying these LC lenses, this dependence needs to be considered as well.

Acknowledgement

The author thanks SANAYI System Co., Ltd for the help with TechWiz 2D software.

References

[1] Okoshi, T. *Three Dimensional Images Techniques*; Academic Press: New York, 1976.
[2] Javidi, B.; Okano, F. *Three-Dimensional Television, Video, and Display Technologies*; Springer: Berlin, 2002.
[3] Son, J.Y.; Javidi, B. *J. Display Tech.* **2005**, *1*, 125–140.
[4] www.3dmovielist.com (accessed July 2011).
[5] Kowel, S.T.; Cleverly, D.S.; Kornriech, P.G. *Appl. Opt.* **1984**, *23*, 278–289.
[6] Ren, H.W.; Fan, Y.H.; Gauza, S.; Wu, S.T. *Jpn. J. Appl. Phys.* **2004**, *43*, 652–653.
[7] Lin, Y.H.; Ren, H; Fan-Chiang, K.H.; Choi, W.K.; Gauza, S; Zhu, X; Wu, S.T. *Jpn. J. Appl. Phys.* **2005**, *44*, 243–244.
[8] Woodgate, G.J.; Harrold, J. *J. Soc. Inf. Disp.* **2006**, *14*, 421–426.
[9] Hiddink, M.G.H.; de Zwart, S.T.; Willemsen, O.H.; Dekker, T. *Proc. Soc. Inf. Disp.* **2006**, *37*, 1142–1145.
[10] Krijn, M.P.C.M.; de Zwart, S.T.; de Boer, D.K.G.; Willemsen, O.H.; Sluijter, M. *J. Soc. Inf. Disp.* **2008**, *16*, 847–855.
[11] Hong, H.K.; Jung, S.M.; Lee, B.J.; Shin, H.H. *J. Soc. Inf. Disp*. **2009**, *17*, 399–406.
[12] Lu, J.G.; Sun, X.F.; Song, Y.; Shieh, H.-P.D. *J. Disp. Technol.* **2011**, *7*, 215–219.
[13] van Berkel, C. *Proc. SPIE* **1999**, *3639*, 84–91.
[14] Hong, H.K.; Park, J.; Lee, S.C.; Shin, H.H. *Displays* **2009**, *29*, 512–520.
[15] Hong, H.K. *Liq. Cryst.* **2011**, *38*, 689–696.
[16] Yeh, P.; Gu, C. *Optics of Liquid Crystal Displays*; John Wiley & Sons: Chichester, 1999.
[17] Yang, D.K.; Wu, S.T. *Fundamentals of Liquid Crystal Devices*; John Wiley & Sons: Chichester, 2006.
[18] SANAYI System Co., Ltd, http://www.sanayisystem.com(accessed July 2011).